International Journal of Research and Reviews in Applied Sciences
ISSN: 2076-734X, EISSN: 2076-7366
Volume 1, Issue 3(December 2009)

COMPARISON OF HYDRODYNAMIC AND MONTE CARLO SIMULATION OF ELECTRON TRANSPORT IN SUBMICROMETRE n^+nn^+ SiC STRUCTURE

H. Arabshahi

Physics Department, Ferdowsi University of Mashhad, Mashhad, Iran

ABSTRACT

A hydrodynamic approach based on velocity and energy conservation equations is developed and used for the simultaneous evaluation of the electronic steady-state transport in an n+nn+ SiC structure. An original decomposition of velocity and energy profiles along the structure in terms of field, convective and diffusion contributions is presented. Monte Carlo simulation of electron transport in this device has also carried out. The anode voltage ranges from 10 to 50 V. The distributions of electron energies and electron velocities, and the profiles of the electron density, electric field and average electron velocity are computed. Based on these data, the excellent agreement of the hydrodynamic approach with Monte Carlo simulations is discussed.

KEY WORDS: *Hydrodynamic; Steady-state transport; Monte Carlo; Anode voltage.*

1. INTRODUCTION:

SiC is a wide bandgap semiconductor, and therefore has a high breakdown field and low thermal generation rate. These properties combined with good thermal conductivity and stability make SiC an attractive material for high power, high temperature and radiation harsh environment electronic devices. Monte Carlo simulations predict a peak electron velocity of 3×10^5 ms^{-1} and a saturation electron velocity of 1.3×10^5 ms^{-1} [1-3]. This makes possible high frequency operation of SiC devices. The improvement in the performance of SiC devices is strongly related to the down-sizing of devices towards the nanometric length scale. This is particularly emphasized for the case of high-frequency operations in the terahertz region. The complexity of the geometries and the extreme conditions due to the ultra-short space/time scales involved give device modeling a crucial role in the research and development of these advanced structures [4-6]. In recent years, various theoretical approaches have been developed and used to calculate electronic transport characteristics in semiconductor devices. Among these methods the hydrodynamic approach, which combines the simplicity of the drift-diffusion model with the possibility of accounting for non-local effects, such as velocity overshoot, has emerged as a very reliable technique [7-10]. In general, the hydrodynamic description is based on velocity and energy conservation equations which are derived from the Boltzmann kinetic equation. However, such a derivation implies the introduction of several assumptions to close the system of conservation equations and, as a consequence, there exists a certain degree of freedom in the choice of the parameters to be used. The aim of this paper is to apply the hydrodynamic model to the case of submicron n^+nn^+ SiC structures. The comparison between the hydrodynamic model model and a Monte Carlo simulation is taken as a validating proof of the hydrodynamic model. In particular, an original decomposition procedure involving the velocity and energy profiles in terms of field, convective and diffusive components has enabled us to carry out a detailed interpretation of electron transport in submicron n^+nn^+ diode. The paper is organized as follows. The theoretical model is briefly surveyed in section 2. The application of the method to the case of SiC diode and some concluding remarks are reported in section 3.

2. METHOD OF CALCULATIONS:

For a one-dimensional geometry, the hydrodynamic approach model equations consist of the continuity equation

$$\frac{\partial n}{\partial t} + \nabla . j = 0 \qquad (1)$$

for negligible charge carrier generation and recombination, the momentum balance equation given by

$$\frac{\partial p}{\partial t} + (\nabla p)v + (p\nabla)v = -enE - \nabla(nkT) - \frac{p}{\tau_p} \qquad (2)$$

or alternatively (only for *x*-component)

$$\frac{[m^*(\varepsilon')nv_x]}{\partial t} + \nabla[m^*(\varepsilon')nv_x v] = -qnE_x - \frac{\partial(nkT)}{\partial x} - \frac{m^*(\varepsilon')nv_x}{\tau_p(t')} \qquad (3)$$

and the energy balance equation is

$$\frac{\partial \varepsilon}{\partial t} + \nabla(v\varepsilon) = -qnvE - \nabla(nkTv) - \nabla(-k\nabla T) - \frac{\varepsilon - 3/2nkT_l}{\tau_\varepsilon(\varepsilon')} \qquad (4)$$

where n, ε ($\varepsilon'=\varepsilon/n$), and v are the electron density, the electron energy density (average electron energy) and the electron drift velocity, respectively. v_x is the x-component of the electron drift velocity and $p=m^*nv$ is the momentum density. Corresponding equations are valid for the y and z components. T is the electron temperature and $\varepsilon'_0=3/2kT_l$ is the average termal equilibrium energy of electrons, where T_l is the lattice temperature. The electronic current density j inside the active device is $j=-nev$, so the total current density is

$$j_t = -nev + \varepsilon_0\varepsilon_r \frac{\partial E}{\partial t} \qquad (5)$$

The momentum relaxation time $\tau_p(\varepsilon')$ is related to the mobility of the electrons via $\mu(\varepsilon')=e/m^*(\varepsilon')\,\tau_p(\varepsilon')$, and the energy relaxation time $\tau_p(\varepsilon')$ describes the exchange of energy between the heated electron gas and the lattice. τ_p and τ_ε and the effective electron mass m^* are assumed to be functions of the mean electron energy. The hydrodynamic equations, together with Poisson's equation

$$\Delta\phi = \nabla E = -\frac{e}{\varepsilon_0\varepsilon_r}(N_d^+ - n) \qquad (6)$$

form a complete set of equations that can be used to solve for the electron density, velocity, energy and electric field for given boundary conditions.

The hydrodynamic model based on equations 1-4 has an evident advantage in that it gives the possibility of verifying directly the assumptions used to close the system of conservation equations. Indeed, the spatial profiles of both velocity and energy can be directly calculated with the Monte Carlo simulation for the structure investigated and compared with those which can be deduced from the hydrodynamic calculations.

Self-consistent Monte Carlo simulation was performed using an analytical band structure model consisting of three non-parabolic ellipsoidal valleys [11-14]. The scattering mechanisms considered in the model are acoustic, polar optical, ionized impurity, piezoelectric and nonequivalent intervalley scattering. The nonequivalent intervalley scattering is between the Γ, *U* and *K*. Acoustic and piezoelectric scattering are assumed elastic and the absorption and emission rates are combined under the equipartition approximation, which is valid for lattice temperatures above 77 K. Elastic ionised impurity scattering is described using the screened Coulomb potential of the Brooks-Herring model.

Steady-state results of high field transport studies have been obtained for lattice temperatures up to 300 K, in order to gain some insight into the hot carrier transport and the energy distribution function that would be generated in the gate-drain region of a power field effect transistor. The input parameters used in the present hydrodynamic and Monte Carlo models for wurtzite SiC are listed in table 1.

	SiC
Density ρ (kgm^{-3})	3200
Longitudinal sound velocity v_s (ms^{-1})	1373
Low-frequency dielectric constant ε_s	9.7
High-frequency dielectric constant ε_∞	6.5
Acoustic deformation potential D(eV)	15
Polar optical phonon energy (eV)	0.012
Band gap (meV)	3.2
Electron effective mass (m_0)	0.28

Table 1: Important parameters used in our hydrodynamic and Monte Carlo model for SiC material [15-16].

The overall diode length which is used in both hydrodynamic and Monte Carlo model has 1 μm in the *x*-direction. A lightly doped active layer (*n*-layer) is sandwiched between cathode and anode layers, which are abruptly doped with a donor density of 10^{24} m^{-3} [17]. The length of the active layer is 0.3 μm. Approximately 10^4 particles are used in the simulation and calculations are performed at room temperature. The applied anode voltage V_a is varied between 10 and 50 V to investigate the effects of field variations on the transport properties. This range of voltages is large enough that velocity overshoot and intervalley transfer effects occur.

3. RESULTS AND DISCUSSION:

The electron concentration and electric field profiles calculated with the hydrodynamic and Monte Carlo models are presented in figures 1a and 1b, respectively. An excellent agreement between the results of the two approaches is found. By comparing the value of the electron concentration through the device, we conclude that the electrons diffuse from the cathode and anode into the active layer and are accelerated towards the anode by the field. The resulting space charge causes the departure from a uniform electric field clearly apparent in figure 1b.

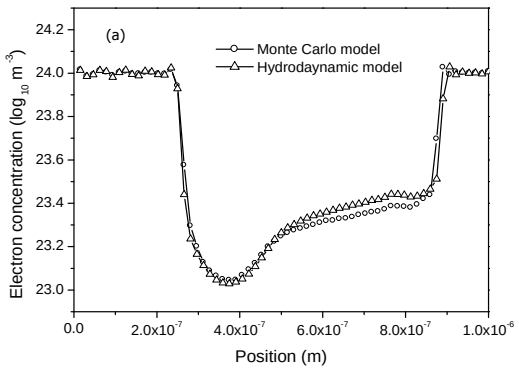

Figure 1: (a) Spatial profiles of electron concentration.

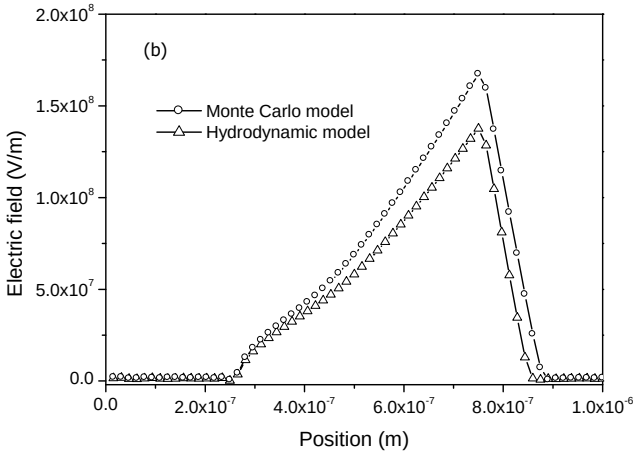

Figure 1: (b) Spatial profiles of electric field calculated with Monte Carlo and hydrodaynamic approaches for the 0.3-0.5-0.2 μm SiC n^+nn^+ diode with doping levels $n=10^{21}$ m^{-3} and $n^+=10^{24}$ m^{-3}. The applied anode voltage is V_a=50 V and the results are at room temperature.

It is apparent from figure 1b that both hydrodynamic and Monte Carlo models show that essentially all the potential is dropped in the active layer. However, as a result of the inhomogeneous space charge the field does vary substantially with position, resulting a maximum magnitude near the anode.

As the next step, figures 2a and 2b give the comparison between the hydrodynamic and Monte Carlo calculations for the velocity and energy profiles. Even in this case a good agreement between the two approaches is achieved. Figure 2a shows that the average drift velocity in the active layer has a maximum value of about 2.4×10^5 ms^{-1} at 300 K. The plot of average electron kinetic energy across the device (figure 2b) provides further information on the dynamics. The electrons reach an average energy between 1.6 and 1.8 eV near the anode region and the more energetic electrons in the distribution have sufficient energy to transfer to the upper valleys.

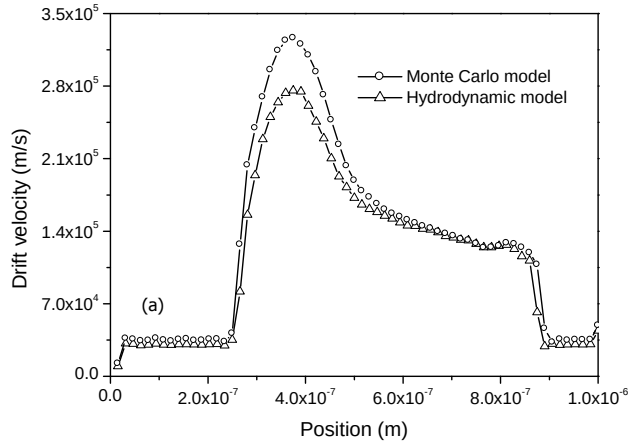

Figure 2: (a) Spatial profiles of drift velocity

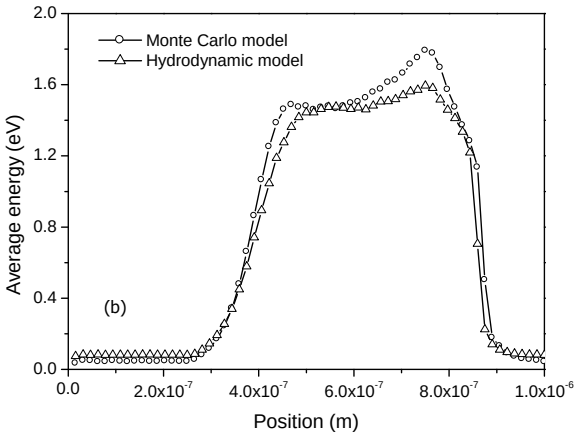

Figure 2: (b) Spatial profiles of electron average energy calculated with Monte Carlo and hydrodaynamic approaches for the 0.3-0.5-0.2 µm SiC n^+nn^+ diode with doping levels $n=10^{21}$ m^{-3} and $n^+=10^{24}$ m^{-3}. The applied anode voltage is V_a=50 V and the results are at room temperature.

Figure 3a and 3b shows the distribution of energy and velocity parallel to the electric field throughout the SiC n^+nn^+ SiC diode in the steady-state at 300 K with a bias of 50 V when the active layer doping level is 10^{22} m^{-3}. It is apparent that there is a significant concentration in the satellite valleys on the anode side of the active layer. These electrons have attained enough energy under the action of the electric field to be scattered into satellite valleys.

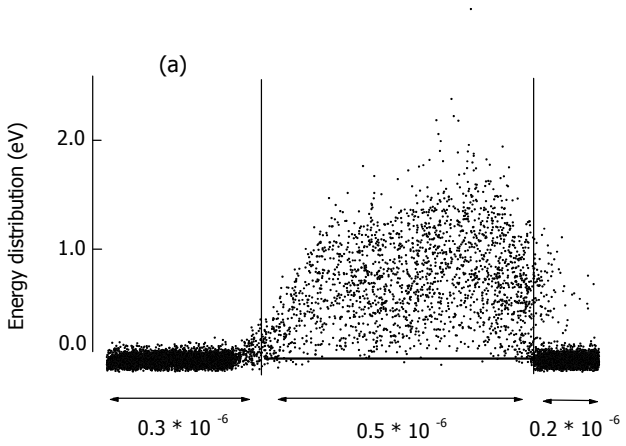

Figure 3: (a) Energy distribution.

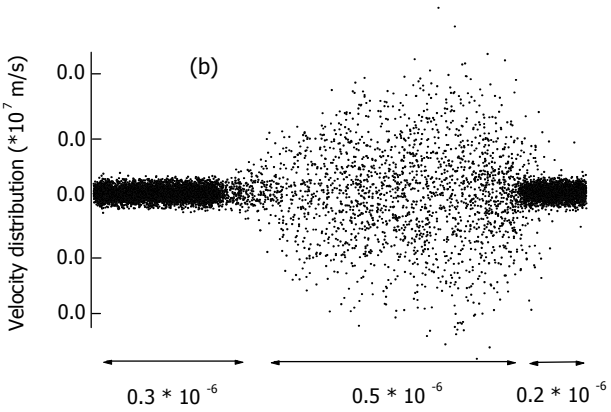

Figure 3: (b) velocity distribution throughout the simulated SiC n+nn+ diode. The applied anode voltage is V_a=50 V and the results are at room temperature.

4. CONCLUSIONS

We have developed a hydrodynamic approach able to evaluate consistently stationary transport in a submicrometre n+nn+ SiC structure at room temperature. The approach has been validated by comparison with a Monte Carlo particle simulator. An original decomposition of electron velocity and energy profiles in terms of field, convective and diffusive contributions has evidenced their importance and their mutual balancing near the homojunctions. The electrons injected from the cathode initially travel quasi-ballistically but there is substantial transfer to the upper satellite valleys as the anode is approached, resulting in a reduced average electron velocity in that region. The peak drift velocity ranges from 2.2×10^5 ms^{-1} to 2.8×10^5 ms^{-1}, with a donor density of 10^{21} m^{-3} and an active layer length of 0.5 μm.

ACKNOWLEDGEMENTS

I would like to thank M. G. Paezi for her useful comments.

REFERENCES

[1] R. Mickevicius and J. H. Zhao, *J. Appl. Phys.*, **83**, 3161 (1998)
[2] R. J. Trew and M. W. Shin, *Third Int. Conf. on Integrated Nonlinear Microwave and Millimeterwave Circuits Dig.*, 109 (1994)
[3] K. Dohnke, R. Rupp, D. Peters, J. Volkl and D. Stephani, *Institute of Physics Conf. Series, IOP Publishing*, Bristol, UK, 625 (1994)
[4] A. K. Agarwal, *The Second Int. Electric Electronic Combat Vehicle Conf. AECV-II*, Dearborn, MI, (1997)
[5] R. P. Joshi, *J. Appl. Phys.* **78**, 5518 (1995)
[6] H. E. Nilsson, U. Sannemo and C. S. Petersson, *J. Appl. Phys*. **80**, 3365 (1996)
[7] K. Blotekjaer, *IEEE Trans. Electron Dev*. **17** 38 (1970)
[8] C. L. Gardner, *IEEE Trans. Electron Dev*. **38** 392 (1991)
[9] Y. K. Feng and A. Hintz, *IEEE Trans. Electron Dev*. **35** 1419 (1988)
[10] M. A. Alsunaidi, S. M. Hammadi and S. M. El-Ghazaly, *Int. J. Num. Mod.: Newt. Dev. Fields*. **10** 107 (1997)
[11] C. Moglestue, *Monte Carlo Simulation of Semiconductor Devices* 1993 pub. Chapman and

Hall
[12] C. Jacoboni and P. Lugli, *The Monte Carlo Method for semiconductor and Device Simulation* 1989 pub. Springer-Verlag
[13] H. Arabshahi, M. R. Benam and B. Salahi, *Modern Physics Letters B*. **21**, 1715 (2007)
[14] H. Arabshahi, *Modern Physics Letters B*. **21**, 199 (2007)
[15] K. Shimada, T. Sota and K. Suzuki, *J. Appl. Phys*., **84** 4951 (1998)
[16] R. P. Joshi, *Appl. Phys. Lett.*, **64**, 223 (1994)
[17] H. Arabshahi, *Modern Physics Letters B*. **21**, 287 (2007)